Characterization of Photoinduced Electron Transfer in Jet-Formed Acceptor−Donor Complexes. 1. Isomeric Forms of Complexes of Anthracene with Aniline Derivatives

A. Tramer,[†] V. Brenner,[‡] P. Millié,[‡] and F. Piuzzi*[,‡]

CNRS Laboratoire de Photophysique Moléculaire Bat. 213, Université Paris Sud, 91405 Orsay cedex, France, and CEA-CEN Saclay DRECAM-SPAM Bat. 522, 91191 Gif sur Yvette cedex, France

Received: October 21, 1997; In Final Form: December 19, 1997

The existence of isomeric forms of donor−acceptor complexes formed in the supersonic expansion was evidenced by their fluorescence, fluorescence excitation, and hole-burning spectra. For each complex, we observed two types of isomers: one E-isomer with broad structureless excitation spectra yielding diffuse, strongly red-shifted exciplex emission and a number of (one to five) R-isomers with narrow band excitation spectra yielding a resonant emission upon the excitation of the lowest vibrational levels of the excited electronic state and exciplex emission from higher levels. A detailed analysis of their excitation spectra (spectral shifts, vibrational structures, bandwidths) is given. The shape of the ground-state potential energy surface (depths and positions of the energy minima, heights of energy barriers, etc.) was determined by calculations involving the "exchange perturbation" treatment and simulated annealing method. The relation between the properties of observed species and calculated configurations is discussed.

I. Introduction

We are interested in the mechanism of the electron transfer (ET) between electron donor (D) and electron acceptor (A) in an isolated, jet-cooled molecular complex AD induced from the optical excitation of one of its components (the electron acceptor in the complexes under study). This process may be described as a radiationless transition from the locally excited state A*D to the ionic state A^-D^+: A*D ⇝ A^-D^+. Its signature is the replacement of the direct (resonant) fluorescence from the initially excited state A*D → AD by the strongly red-shifted exciplex emission A^-D^+ → AD. We chose for this study a family of complexes involving the same electron acceptor, anthracene, and a group of donors slightly differing by their properties: *N*,*N*-dimethyl-aniline and its derivatives or analogues.

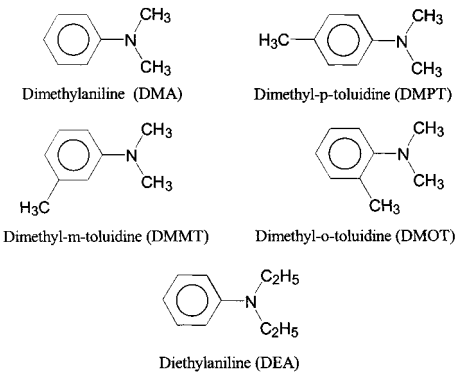

The reasons of our choice are obvious: the anthracene−alkylaniline systems have been studied in the pioneering works of Weller and his co-workers on electron transfer and exciplex formation in fluid solutions.[1,2] On the other hand, bichromophoric systems involving anthracene and aniline derivatives linked by a flexible aliphatic bridge became objects of a number of studies carried out in condensed phases and in supersonic jets.[3−5]

Preliminary results of this work have been previously published.[6,7] Prior to the discussion of the ET mechanism given in the second part (denoted as 2) of this series, it is necessary to determine the number and essential parameters of isomeric forms of individual AD complexes.

The existence of isomeric forms is a rule for such systems: the studies carried out in supersonic jets allowed to demonstrate the presence of isomers in such systems as van der Waals complexes of aromatics with simple molecules,[8,9] dimers of aromatics[10,11] or small clusters involving an aromatic molecule and a few rare gas atoms.[12,13] The presence of different isomers may easily be deduced from the electronic spectra of jet-cooled complexes, but the only technique allowing to separate unambiguously spectral features belonging to each isomer and determine the number and relative concentrations of individual species in the mixture is the hole-burning (or selective level depletion) spectroscopy.[14]

The existence of the isomeric forms of molecular complexes reflects the complexity of their potential energy surfaces (PESs). It is, therefore, important to complete the experiment by calculations of their PESs. These surfaces are usually complicated and contain a large number of minima. We expect that the deepest ones, separated by nonnegligible energy barriers, correspond to the observed isomeric forms.

The scope of this work, involving both experiment and modeling, is to check which parameters determine the number and structures of isomeric forms in this series of complexes. By combining the hole-burning spectroscopy (HBS) with a study of the excitation spectra of individual emission components, we separated the spectral features of each isomeric form of five different AD complexes. On the other hand, we determined, by independent calculations, the geometry and depth of the energy minima of the ground-state energy surface for

[†] CNRS Laboratoire de Photophysique Moléculaire.
[‡] CEA-CEN Saclay DRECAM-SPAM.

S1089-5639(97)03388-4 CCC: $15.00
Published on Web 04/08/1998

each complex. Finally, we tried to establish a relationship between computed configurations and observed species.

II. Methodology

A. Experimental Procedures. All experiments are performed in a pulsed supersonic expansion using a general valve nozzle and helium as the carrier gas. The vacuum system is composed of two chambers separated by a skimmer.

In the first chamber, two apertures equipped with light baffles let enter one (for laser induced fluorescence) or two (for hole burning spectroscopy) laser beams which cross with the supersonic jet at a 15 mm distance from the nozzle. The beams are issued from two Lambda Physik FL 2002 dye lasers with a ca. 0.2 cm^{-1} line width pumped by one (or two when a large delay is needed) Lambda Physik excimer lasers. The fluorescence light is collected by a *f*:50 mm lens and passed through a small Bausch and Lomb monochromator with widely open ($\sim$1000 cm^{-1}) slits set at 370 nm for detection of the resonant fluorescence or at 450 nm for the exciplex emission. The excitation spectra of resonant fluorescence and exciplex fluorescence, respectively denoted as FES-R and FES-E, were recorded by scanning the laser through the initial part of the absorption spectrum containing its origin (0_0^0) band and the $0_0^0 + 385$ cm^{-1} band involving the ν_{12} mode of anthracene. For the hole-burning experiment, we used an intense (200−400 μJ/pulse) pump beam which was scanned across the same spectral region while the weak ($\sim$20 μJ/pulse) probe beam was fixed at a frequency corresponding with one of the strong bands in the fluorescence excitation spectrum. Only the emission induced by the probe laser was detected, and in order to get rid of the emission due to the pump laser, the delay between the two pulses was significantly longer than the fluorescence lifetime. In the case of the resonant fluorescence, the lifetime is of the order of 20 ns and pump and probe beams may cross the jet at the same point. For the long lived ($\tau \approx 300$ ns) exciplex emission the spatial displacement of the packet of excited molecule during a ca. 1.5 μs delay is nonnegligible so that the two beams must be separated by 1.6 mm.

Because of the high intensity of the pump beam, the hole-burning spectra are not completely free from saturation effects. In order to reduce them and approach the real intensity ratios of vibronic bands, we took care to use the lowest possible pump laser power. We prefer, nevertheless, to use the data from fluorescence excitation spectra in the discussion of the intensity distribution.

The second chamber is equipped with a time of flight mass spectrometer, contains two apertures for excitation and ionization laser beams, and is used for the recording of mass-resolved REMPI spectra.

B. Modeling. The molecular complexes are bound by weak intermolecular forces. Different components of the interaction energy (electrostatic, polarization, dispersion, and repulsion) vary in different way with the configuration of the interacting pair so that the equilibrium structures of the different isomers often result from the balance between opposite tendencies (mainly from the balance between electrostatic and dispersion interactions). Consequently, the model for intermolecular interactions must be sufficiently precise to reproduce the correct balance between the different energy components and, at the same time, relatively simple to allow an exhaustive exploration of the potential energy surface.

The model used here—a semiempirical method developed by Claverie and based on the "exchange perturbation" theory—has been already described in detail;[15] therefore, we will give only its main characteristics. At the second order of the perturbation treatment, the interaction energy is a sum of four terms: electrostatic, polarization, dispersion, and short-range repulsion. Each contribution is expressed by simplified analytical formulas which give a reliable description of interactions for all intermolecular distances.

The dispersion and repulsion terms are computed as sum of atom−atom contributions; the repulsion term includes the variation of the van der Waals radius of each atom with its charge within each molecule.[16] Empirical atomic parameters involved in these two terms reproduce the results obtained for small systems by both *ab initio* and symmetry-adapted perturbation calculations.[17] Furthermore, they have been determined in such a way so as to be transferable.

The electrostatic term is calculated as the sum of multipole−multipole interactions. The set of multipoles of each molecular subunit (a monopole, a dipole, and a quadrupole on each atom and one point per chemical bond) is obtained by the procedure developed by Vigné-Maeder et al.[18] From the exact multipolar multicentric development of the electronic distribution derived from the wave function of each molecular subunit, a simplified representation of the multipole distribution is generated through a systematic procedure of the reduction of the number of centers. The wave functions are obtained by *ab initio* self-consistent field calculations performed in a double-ζ basis (6-31G basis set of Pople[19]) with the HONDO program.[20] The geometry of the molecules are either experimental or, in the absence of reliable experimental data, optimized by the AM1 method.[21] We assume that these geometry remain unchanged by complex formation; this approximation will be further discussed in section III.B1. The polarization term is based on the same multipole expansion as above, plus experimental atom- and bond-polarizability increments. The charge transfer term, negligible for systems in their ground electronic state, was not included.

This model is completely independent of the experiment and does not imply any fitting parameter. It is suited for the study of clusters in their ground electronic states and it has already been successfully applied to different systems.[22] With some modifications, it can be applied to clusters in their excited or ionic electronic states. These modifications and their validity will be discussed in part 2 of this paper.

Investigation of the potential energy surfaces (i.e., the localization of the stationary points minima and saddle points) are performed by two different procedures. Efficient determination of minima is ensured by a combination of global (simulated annealing)[23] and local (quasi-Newton)[24] methods. This procedure, similar to that used by Liotard et al.,[25] is an extension of the simulated annealing method applied to complicated PESs involving many minima. First, a random search on the PES is performed using the Metropolis algorithm.[26] The configurations obtained from this exploration are then sorted out and optimized by a local minimization method. Finally, it is checked that all extrema found in this way correspond to energy minima by scrutinizing the eigenvalues of their hessian.

We call occurrence the number of times that each minimum is detected. The ratio between occurrences of two minima reflects roughly the difference in the width of their potential wells. Thus, a minimum with narrow well will have low occurrence in our exploration procedure and should correspond to an isomer with low probability of formation. The occurrences will be used in further discussion.

For the characterization of saddle points between the different minima, the local technique developed by Liotard et al.,[27] the "chain method", is used. It consists in shifting on the PES a

path connecting the two minima of interest, the starting path being generated from a user given saddle point and the two minima. The energetic relaxation of the path is performed until the highest point cannot be more relaxed. We have to mention here that the localization of a saddle point between two minima has to be performed with a large set of initial configurations of starting saddle point in order to be practically sure to determine the saddle point of the lowest energy**.**

We obtain in this way a large number of minima, of which only some are significant. We may perform a tentative selection and retain only the minima fulfilling two conditions: (i) they must be separated by energy barriers ΔV such that $\Delta V \gg kT_{\text{vib}}$ and (ii) the absolute value of the interaction energy does not exceed that of the deepest minimum by more than 30% of the total interaction energy.

III. Results

A. Experimental Results. *(1) General.* In all systems under study, the fluorescence spectrum is composed of two kinds of emission bands:

(i) the narrow-band *resonant* (i.e., with the same position of the 0_0^0 band as in absorption) emission with the lifetime close to that of bare anthracene (∼20−25 ns) and (ii) the *exciplex* emission characterized by its strongly red-shifted ($\Delta\nu \approx 4000$ cm $^{-1}$) and diffuse ($\delta\nu \approx 3000$ cm^{-1}) spectrum with a much longer (∼300 ns) decay time.

For each complex, we recorded separately the fluorescence excitation spectra (FES) of both components: the resonant fluorescence (FES-R) and the exciplex fluorescence (FES-E). The FES of our model system, the A-DMA complex, are represented in Figure 1. Both spectra reproduce the coarse features of the spectrum of the bare anthracene molecule but are red shifted by 523 cm^{-1}. Moreover, instead of single 0_0^0, $\overline{11}_0^1 = 0_0^0 + 215$ cm^{-1}, and $12_0^1 = 0_0^0 + 385$ cm^{-1} bands of the free molecule, we observe, associated to each vibronic transition a system of densely spaced, narrow bands and/or broad, structureless bands. The FES-R is composed (beside a few hot bands of free anthracene) uniquely of narrow bands belonging to the 0_0^0 transition, while FES-E contains broad-band features related to the 0_0^0 and 12_0^1 transitions and narrow bands associated to the 12_0^1 transition. The hole-burning spectra (HBS) represented in Figure 1 enable us to separate spectral features corresponding to different molecular species.

The hole-burning spectra show the following in all AD systems: (i) all narrow-band systems belong to an isomeric form called R-isomer. Upon the excitation of the lowest vibronic levels, the fluorescence is *resonant* and corresponds to the direct decay of the initially prepared locally excited A*D state. Upon the excitation of higher levels (e.g., those belonging to the 12_0^1 system), the resonant fluorescence is quenched and only the *exciplex* emission is observed. This indicates that the A*D $\rightarrow$ A$^-$ D$^+$ electron transfer takes place at the time scale much shorter than the 20 ns lifetime of the A*D state. (ii) Broad bands, present uniquely in the excitation spectra of the exciplex fluorescence, are due to an other isomeric species: E-isomer. The absence of the resonant emission indicates that the locally excited A*D state is depopulated with a rate much larger than that of the A*D $\rightarrow$ AD decay. The widths ($\delta\nu \approx 100$ to 170 cm^{-1}) of bands corresponding to the 0_0^0 and 12_0^1 transitions suggest that the initially excited A*D state decays at the subpicosecond time scale by the A*D $\rightsquigarrow$ A$^-$ D$^+$ electron transfer (cf. part 2).

Similar features are observed for other complexes but the narrow-band spectra belong not to one but to a number of different *R*-isomers while there seems to be only one *E*-isomer for each complex (or a few of them but with nearly identical, overlapping broad band spectra).

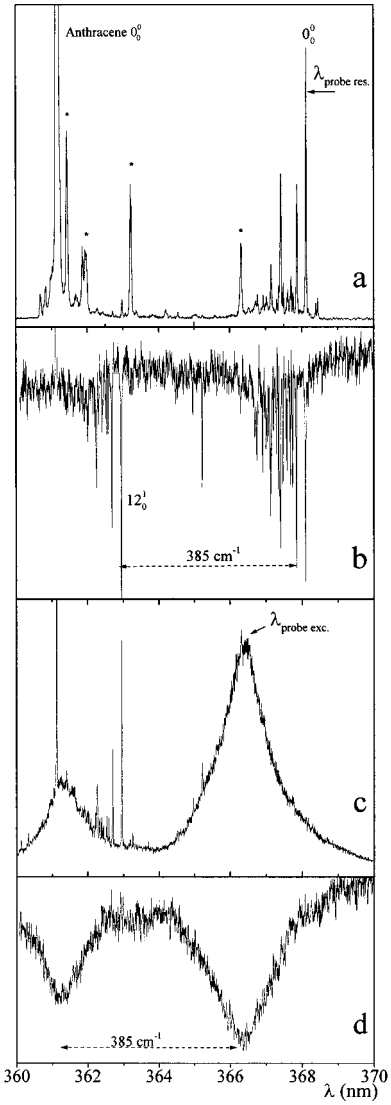

Figure 1. Characterization of the anthracene−dimethylaniline complex absorption: (a) fluorescence excitation spectra with detection of the resonant fluorescence (375 nm region) with "hot" bands of free anthracene marked by *, (b) hole-burning spectra with probe laser fixed on the most intense narrow band and detection of the resonant fluorescence, (c) fluorescence excitation spectra with detection of the exciplex fluorescence (450 nm region), and (d) hole-burning spectra with probe laser fixed on the maximum of the broad exciplex absorption band and detection of the exciplex fluorescence.

Using the mass-selective multiphoton ionization technique (MS/REMPI), one can show that all spectral features belong to 1:1 complexes, the concentration of AD_2 or A_2D species being negligible. As an example, the MS/REMPI spectrum of the A-DMOT 1:1 complex in the 12_0^1 range is compared in Figure 2 with the FES-E. One can show in the same way that the *E*-isomers of A-DMA and A-DEA are also 1:1 complexes.

(2) R-Isomers. The characteristic properties of the different R isomers are given in Table 1. For each complex, R isomers are labeled from 1 to *n*, 1 referring to the system showing the largest spectral red shift.

(a) *Number of isomers.* The number of R isomers varies from one to five and seems to increase when the donor structure becomes more complicated: one R isomer for the complex involving the simplest DMA donor and two for only slightly

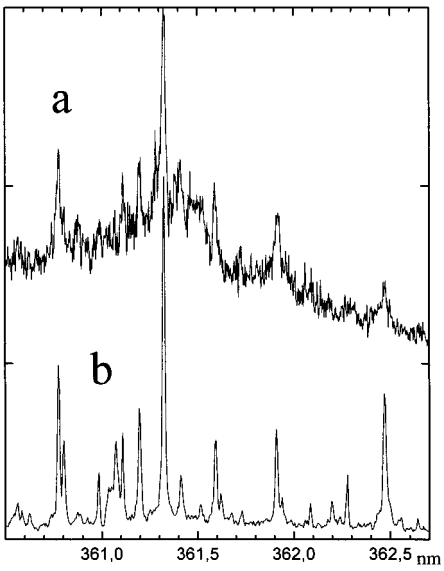

Figure 2. Comparison of the MS/REMPI spectrum (a) and FES-E (b) of the 1:1 anthracene−dimethyl-*o*-toluidine complex in the 12_0^1 range.

modified structures of DMPT and DMMT, while their number is increased to three for DEA and to five for the DMOT molecule which shows strong steric hindrance effects.

(b) *Spectral shifts of fluorescence excitation spectra.* The red shifts $\Delta\nu$ of the 0_0^0 bands of R isomers with respect to the 0_0^0 transition of the bare anthracene molecule vary over a wide range (400−680 cm^{-1}). It is interesting to note that the shifts are almost identical for both R isomers of A-DMPT ($\Delta\nu_1 - \Delta\nu_2 = 8$ cm^{-1}) and A-DMMT ($\Delta\nu_1 - \Delta\nu_2 = 13$ cm^{-1}) while in the case of DMOT complexes $\Delta\nu_1 - \Delta\nu_5$ amounts to ∼300 cm^{-1} . The case of DEA complexes is peculiar: the red shifts of R_1 and R_2 differ only by 2 cm^{-1} while that of R_3 is smaller by 50 cm^{-1}. Only for the DEA and DMOT complexes do we observe red shifts as large as 650−680 cm^{-1} and as small as 396 cm^{-1}, while for all others they are contained in the 490−585 cm^{-1} limits. We are not able to correlate the frequency shifts with other properties of different isomeric forms.

(c) *Vibrational structure of fluorescence excitation spectra.* The vibrational structure of the band systems corresponding to the 0_0^0 and 12_0^1 transitions, and extending over ca. 100−150 cm^{-1} range, involves external (intermolecular) modes. Two typical HBS (those of R_4 and R_5 isomers of A-DMOT complex) are represented in Figure 3 and the corresponding frequency intervals are listed in Tables 2 and 3 with tentative vibrational assignments. An unambiguous vibrational analysis cannot be proposed because of a strong congestion and a large number of doublets probably due to Fermi resonances in the $\Delta\nu > 40$ cm^{-1} range. For this reason, the assignment of stretching modes expected in the 40−60 cm^{-1} range is uncertain and we give in Table 1 only the distances between the 0_0^0 and first ($\Delta\nu < 35$ cm^{-1}) bands in the spectra of different isomers; these frequencies must be those of low-frequency external modes. We may draw some qualitative information from this analysis: (i) a large number of active modes (four or five of them appear while the overall number of external modes is equal to six) and a presence of numerous combination bands, (ii) relatively short vibrational progressions ($\Delta v \leq 2$) with the maximum intensity in the origin band; the only exception is the R_1 isomer of the A-DMOT showing a much longer progression with a displaced intensity maximum.

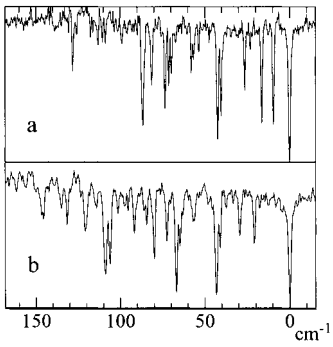

Figure 3. Hole-burning spectra of (a) R_4 isomer and (b) R_5 isomer of the anthracene−dimethyl-*o*-toluidine complex with the probe laser fixed respectively on the 0_0^0 band of each isomer and with detection of the resonant fluorescence.

These features suggest a low symmetry of the system (absence of strong selection rules) and a difference between equilibrium configuration of the ground and excited state corresponding to small displacements along several intermolecular coordinates.

TABLE 1: Spectroscopic Characteristics (expressed in cm^{-1}) of the *R*-type Isomers of the Different Complexes[a]

	isomer				
complex	R_1	R_2	R_3	R_4	R_5
A-DMA					
$\delta\nu$	523				
external modes	19.4, 27.3, 31.6				
A-DMPT					
$\delta\nu$	583	575			
relative population	100	≈30			
external modes	18.0, 24.4, 29.5, 35.1	19.0, 27.0, 33.0, 35.5			
A-DMMT					
$\delta\nu$	553	540			
relative population	100	≈50			
external modes	19.1, 27.7, 31.6, 34.9	15,9, 17.8, 22.0, 24.2, 27.2			
A-DMOT					
$\delta\nu$	678	552	524	493	396
relative population	≈5	≈15	≈15	≈70	100
external modes	18.8, 22.0, 25.6, 31.6	17.7, 23.4, 31.3	24.8, 26.9, 31.1	21.2, 29.7	9.6, 16.5, 23.5
A-DEA					
$\delta\nu$	650	648	598		
relative population	≈25	≈75	≈100		
external modes	17.4, 23.9, 26.6, 32.9, 34.6	22.2, 26.8, 33.1	14.2, 20.1, 23.6, 28.8, 31.8		

[a] Expressed in cm^{-1}. $\delta\nu$ red shift of the isomer origin band with respect to anthracene 0_0^0, relative population of *R*-isomers with respect to the isomer of highest population, and frequencies of the external modes (limited to external modes with $\nu < 35$ cm^{-1}).

TABLE 2: Vibrational Analysis of the Fluorescence Excitation Spectrum of the R_4 Isomer[a]

R_4 isomer				
$\upsilon_0 = 27201\ cm^{-1}$ and $\delta\upsilon = 493\ cm^{-1}$				
$\upsilon - \upsilon_0$	I	attribution	FES-R	FES-E
0.0	100	0_0^0	vs[b]	m
21.2	5	a_0^1	s	m
29.7	9	b_0^1	w	vw
41.5	13	Fermi resonance $a_0^2 - c_0^1$?	w	w
43.8	100		w	s
57.4		b_0^2	w	w
65.5	13	Fermi resonance $c_0^1\, a_0^1 - d_0^1$?	w	w
67.5	80		w	s
73.3	13	$c_0^1\, b_0^1$	vw	w
81.0	36	e_0^1?	vw	m
85.8	29	c_0^2?		
93.0	11	$a_0^1\, b_0^1\, c_0^1$?		
96.6	7	$d_0^1\, b_0^1$?		
98.7	5	$a_0^1\, c_0^2$?		
102.9	4	$a_0^1\, e_0^1$?		
107.4	29	$d_0^1\, a_0^2$?		
110.4	34	$c_0^1\, d_0^1$?		
115.9	4	$a_0^1\, b_0^1\, d_0^1$?		
122.0	11	$e_0^1\, c_0^1$?		
133.5		d_0^2?		
152.0		$d_0^1\, c_0^2$?		
174.0		$d_0^2\, c_0^1$?		

[a] Intensities of the bands in resonant and exciplex domain are given for comparison purposes. Note that the intensities are from the FES-E spectrum. The origin band is emitting dual fluorescence, and then its intensity could not be taken as reference for normalization. The intensity of the band at 43.8 cm^{-1} was thus taken as reference. [b] vs = very strong. s = strong. m = medium. w = weak. vw = very weak.

The characteristic frequencies of different complexes are close together: they are nearly identical for the R isomer of A-DMA, the R_1 isomer of DMMT, and the R_2 isomer of DMPT. On the other hand, exceptionally low frequencies appear in the spectra of the R_5 isomer of A-DMOT and the R_3 isomer of A-DEA.[36]

It is interesting to note that the "hot" bands of AD complexes are practically absent in the spectra of all systems. In view of the low frequencies of external modes, it indicates the vibrational temperature for external modes of the complexes $T_{vib} < 10$ K.

(d) *Rotational contours of bands.* The contours recorded with the spectral resolution limited by the laser spectral width of 0.2 cm^{-1} are significantly different from that of the origin band of the bare anthracene molecule (Figure 4a) with a 1.4 cm^{-1} width and a central dip characteristic for the B-type rotational envelope. For example, the contour of the origin band of the A-DMA complex (Figure 4b) does not present any central dip and is narrower ($\sim$1.0 cm^{-1}). This is obviously due to a larger moment of inertia of the complex and to the different orientation of the transition moment with respect to the inertia axes (we implicitly assume that the rotational temperature is the same for all isomers). Some differences between contours of the origin band of different isomers are also noticed. The most striking example is that of R_1 and R_2 isomers of the A-DMPT complex with 0.3 and 1.1 cm^{-1} widths, the first one being probably limited by the instrumental width. Our resolution is, unfortunately, too low for a detailed study of band shapes and widths.

We did not notice any significant differences between the widths of the origin bands of the 0_0^0 and 12_0^1 or 12_0^2 band systems (Figure 4c).

TABLE 3: Vibrational Analysis of the R_5 Isomer[a]

R_5 isomer				
$\upsilon_0 = 27299\ cm^{-1}$ and $\delta\upsilon = 396\ cm^{-1}$				
$\upsilon - \upsilon_0$	I	attribution	FES-R	FES-E
0.0	100	0_0^0	s[b]	
9.6	61	a_0^1	s	
16.5	59	b_0^1	s	
23.5	12	c_0^1	vw	
26.5	43	$a_0^1\, b_0^1$?	s	
40.8	68	d_0^1	s	
43.0	76	e_0^1	s	
54.3	20	$a_0^2\, b_0^2$?	m	
57.3	23	$d_0^1\, b_0^1$?	m	
58.7	24	$e_0^1\, b_0^1$?		
61.0	10	$d_0^1\, a_0^2$, $e_0^1\, a_0^2$?		
68.4	8	$d_0^1\, a_0^1\, b_0^1$?		
70.6	33	$e_0^1\, a_0^1\, b_0^1$?		
72.3	40	$d_0^1\, b_0^2$?		
74.5	51	$e_0^1\, b_0^2$?	s	w
82.6	41	$d_0^1\, e_0^1\, d_0^2$?	m	w
88.0	61	e_0^2?	s	w
100.6	15	$e_0^2\, b_0^1$?	w	w
110.7	11	$e_0^2\, c_0^1$?	w	w
112.5	11	$e_0^1\, d_0^1\, a_0^2$?		
115.1	17	$d_0^2\, c_0^1$?		
117.2	8	$e_0^1\, d_0^1\, b_0^2$?		
119.6	11	$e_0^2\, b_0^2$?		
128.4	11	$e_0^2\, d_0^1$?		
130.6	27	e_0^3?		

[a] Intensities of the bands in resonant and exciplex emission domain are given for comparison purpose. Intensities are measured in the hole-burning spectrum. [b] s = strong. m = medium. w = weak. vw = very weak.

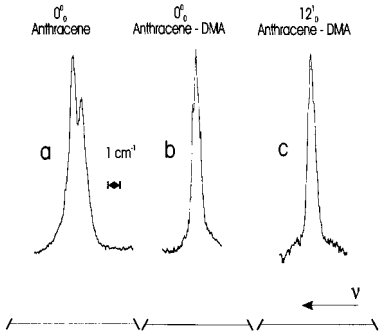

Figure 4. Rotational contour of (a) 0_0^0 band of bare anthracene, (b) 0_0^0 band, and (c) 12_0^1 band of the anthracene−dimethylaniline complex.

(3) E-Isomers. As already said, the hole-burning spectra suggest that there is only one E-isomer for each complex. The bands of E isomers are structureless with the shapes varying, for different complexes, between quasi-Gaussian and quasi-Lorentzian forms. As will be discussed in part 2, one can consider them as the envelopes of vibrational progressions such as those of R type isomers but unresolved because of a strong homogeneous broadening of individual transitions. The Gaussian shape is expected when the widths of individual transitions are of the same order of magnitude as their intervals; the contour of the resulting broad band reflects the intensity distribution in the progression. On the other hand, when the broadening is so

TABLE 4: Spectroscopic Characteristics of the *E*-Isomers of the Different Complexes[a]

complex	A-DMA	A-DMPT	A-DMMT	A-DMOT	A-DEA
$\delta\nu$; $\Delta\nu$ (cm^{-1})	−395, 100	−390, 170	−425, 145	−400, 100	−470, 100
ν_{max} (nm)	450	480	460	455	460
(cm^{-1})	22200	20850	21750	22000	21750
τ (ns)	280	300	190	200	300
EI (eV)	7.12[30]	6.95[31]	7.06[31]	7.40[31]	6.95[32]

[a] Spectral shift ($\delta\nu = \nu_{max} - \nu_o$), full width at half-maximum ($\Delta\nu$) of the 0_0^0 band, maximum of exciplex emission (ν_{max}), lifetime of this emission (τ), and ionization energy of the donor molecule (EI).

strong that the individual widths are as large as the overall extension of the band system, the band shape becomes closer to the Lorentzian form.

The spectroscopic and dynamic characteristics of the E-isomers are listed in Table 4. The red shifts of E-isomer spectra are smaller than those of R isomers, in the 380−450 cm^{-1} limits. It is, however, important to note that we refer here to the position of the absorption maximum instead of the 0_0^0 band.

(4) Intensities and Populations. We observe in the excitation spectra of the overall resonant fluorescence (sum of emission components due to all R isomers of a given complex) important differences between intensities of band systems due to each isomer. Since the fluorescence decay times are nearly the same for most of the systems, one can assume that their fluorescence yields are identical. If it is so, the relative intensities reflect differences in the populations of different isomers. They vary from case to case. In the A-DMPT complex, population of R_1 isomer is about three times that of the R_2 one, while in the similar A-DMMT system the population of the R_1 isomer is about twice that of the R_2 one. In the A-DMOT complex, R_5 has the highest population followed by R_4 while the populations of R_1, R_2, and R_3 isomers are very low. At last, among the isomers of the A-DEA system, the population of R_3 and R_2 is higher than that of the R_1 isomer.

The relative populations of the E isomers may be roughly estimated from relative intensities in the 12_0^1 transition: all isomers emit the exciplex fluorescence, so that we can consider that their fluorescence yields are the same. The relative population of the *E*-form estimated in this way varies in very broad limits: it seems to be large in the case of DMA and DMMT complexes, much smaller in complexes of DMPT and DEA. Its relative concentration in the A-DMOT system is so low that the broad band of the E-isomer is completely hidden in the strongly congested spectrum of R-forms; its presence was evidenced only by the REMPI technique.

B. Modeling. *(1) Molecular Structures and NR_2 Inversion.* We will assume that isomers differ by the configuration of the complex (i.e., by the intermolecular coordinates) while only one structure is assumed for each donor. As a matter of fact, the structures of the fluorescence excitation spectra of DMA and DEA may be explained by assuming the existence of a unique species, as shown by Wallace and al.[29] The structure of DMA is well-known and may not be significantly modified by methyl substitution, as evidenced by a slight decrease of the ionization energy from 7.12 eV[30] to 6.95[31] and 7.06[31] eV respectively. The ionization energy of DEA is lowered only to 6.95[32] eV. In contrast, the structure of the DMOT is seriously modified because of the steric hindrance between $N(CH_3)_2$ and ortho CH_3 groups inducing the increase of its ionization energy to 7.40[31] eV.

The structures of the donor molecules are obtained from AM1 calculations, except for DMPT and DMMT, for which we assume the DMA structure with a methyl group replacing a H atom. For DMA, the AM1 calculations give an angle of 26° between the axis of the NR_2 group and its projection at the ring plane, close to the value observed for aniline (38°).[33] One can suppose that this angle remains nearly the same for DMPT and DMMT. For DEA, the angle of 15° is obtained by AM1 calculations. In the DMOT, the steric hindrance between the dimethylamino and ortho methyl substituents induces a rotation of the NR_2 group around the C−N bond by 80°.

Rigid molecular structures not modified by the complex formation were assumed. This assumption creates a difficulty in the case of NR_2 group. In the DMA molecule, the inversion of the NR_2 group leads to two strictly equivalent minima separated by a barrier estimated at 0.55 kcal/mol from calculations[34] and at 0.24 to 0.72 kcal/mol from microwave measurements.[35] In the complex, the symmetry is broken and we have two structures differing by orientation of the $-NR_2$ group pointing either toward anthracene or in the opposite direction (we will note these configurations respectively A← and A→) and by their interaction energies. The barrier between these two configurations corresponds in the case of rigid donors to a rotation of about 180° around their long axis and is high because this on-site rotation is hindered. The same transformation can be realized by the inversion of the NR_2 group which implies a substantially lower barrier. We will illustrate it in the case of A-DMA complex, where the barrier between the two minima is of 1.76 kcal mol^{-1} (∼600 cm^{-1}), if it is assumed that the DMA molecule is rigid. The alternate path involving NR_2 inversion was simulated using the following procedure. The energy of the planar DMA molecule was calculated and found higher by 0.5 kcal/mol than that of the most stable configuration. Then the energies of minima were recalculated using this planar structure: both of them are increased by 0.4 kcal/mol but there is almost no barrier in between. The barrier may thus be roughly estimated as ∼0.9 (0.5 + 0.4) kcal/mol (≈300 cm^{-1}). This approach is also valid for DMPT and DMMT and, to some extent, to DEA where steric hindrance effects occurring between two ethyl substituents in NR_2 group may modify the inversion conditions. The case of DMOT is totally different because its structure is rigid so that the inversion of the NR_2 group is impossible.

(2) Complexes. The overall interaction energies and their components corresponding to the dispersion, electrostatic, polarization, and repulsive terms are given in Table 5 for the minima of the different complexes selected according to the previously defined rules (section IIB). We would like to emphasize the interest of this partition. The total interaction energy is, in many cases, close to the dispersion interaction alone, while the other three terms mutually cancel. The position of the energy minimum may, nevertheless, be determined by the electrostatic and repulsive interactions. This is due to a relative insensitivity of dispersion to details of the intermolecular configuration, while electrostatic interactions are sensitive to the position of the parts of the molecule bearing electric charges or dipoles. To get insight into this effect, for all complexes, we separated the electrostatic term into parts corresponding to

TABLE 5: Decomposition of the Total Interaction Energy in Its Different Components, for the Selected Minima of the Different Complexes[a]

complex	minimum ($n°$)	occurrence of the minimum	total interaction energy	dispersion	electrostatic	polarization	repulsion	NR_2 orientation	similarity with configuration of minimum of A-DMA ($n°$)
A-DMA	1	47	−5.26	−5.85	−1.88	−0.22	2.70	A←	
	2	45	−4.74	−4.82	−2.08	−0.22	2.39	A→	
	3	1	−4.02	−5.11	−0.91	−0.11	2.10		
	4	3	−4.01	5.03	−0.86	−0.26	2.14	A→	
A-DMPT									
	1	23	−5.27	−5.89	−1.86	−0.22	2.70	A←	(1)
	2	35	−5.01	−5.19	−2.13	−0.27	2.58	A→	(2)
	3	12	−4.14	−5.34	−0.86	−0.11	2.17		(3)
	4	2	−4.04	−4.98	−0.91	−0.26	2.17	A→	(4)
A-DMMT									
	1	31	−5.49	−6.21	−1.88	−0.23	2.83	A←	(1)
	2	39	−5.29	−5.45	−2.31	−0.27	2.74	A→	(2)
	3	14	−4.79	−4.83	−2.11	−0.24	2.39	A→	
	4	6	−4.69	−5.81	−1.25	−0.21	2.59	A←	
	5	3	−3.93	−5.10	−0.81	−0.10	2.08		(3)
A-DMOT									
	1	28	−5.11	−6.29	−1.44	−0.19	2.75		
	2	20	−4.93	−5.51	−2.00	−0.18	2.77		
	3	18	−4.59	−5.59	−1.28	−0.18	2.46		
	4	13	−4.06	−5.29	−0.77	−0.12	2.12		
	5	4	−3.94	−5.10	−0.79	−0.11	2.07		
A-DEA									
	1	27	−5.19	−7.06	−0.96	−0.19	3.02	A←	(1)
	2	33	−4.83	−5.16	−1.89	−0.22	2.44	A→	(2)
	3	13	−4.40	−5.51	−1.03	−0.12	2.26		(3)
	4	10	−4.26	−5.55	−0.78	−0.11	2.18	A←	
	5	3	−4.13	−5.60	−0.57	−0.26	2.30	A→	(4)

[a] All energies expressed in kcal/mol. The occurrence of the different minima is expressed in percent of the total number of minima detected. The orientation of the NR_2 group of the donor with respect to the anthracene molecule (toward or in opposite direction) is indicated respectively by A← and A→. The eventual configuration similarity with one of those of the A-DMA complex is indicated by giving the corresponding minimum number.

the different functional groups of the donor (cycle, CH_3, and NR_2). One can deduce therefrom the importance of the orientation of the NR_2 group. The NR_2 pointing toward the anthracene molecule (A←) gives a repulsive contribution to the electrostatic interaction. On the other hand, in the opposite configuration (A→), the NR_2 group gives an attractive contribution.

We obtain a large number of minima and only a few of them are conserved for further discussions. The criteria of this choice were given at the end of section II.B. We also take into account the occurrences of different minima in the simulated annealing "experiment".

In the simplest case of the A-DMA complex, two configurations show a much higher stability and higher occurrences than all others (Table 5): (i) in the most stable configuration (1), the long *L*-axis of DMA forms a ca. 40° angle with the plane of the anthracene molecule, its projection at this plane being nearly parallel to the short *M′*-axis of anthracene. The NR_2 group approaches closely the anthracene molecule (the distance of the N-atom from its center is of 4.6 Å) and points to it (configuration A←) (Figure 5a).

(ii) For the minimum (2) with the interaction energy smaller by 0.5 kcal/mol, the long (*L* and *L′*) axes of both molecules are nearly parallel with the A→ orientation of the NR_2 group while the plane of the DMA ring forms an angle of about 35° with the anthracene plane (Figure 5b).

The energy difference between these two minima is essentially due to the dispersion term which is more important for minimum (1). As previously discussed, the barrier between minima (2) and (1) of 1.76 kcal mol^{-1} (∼600 cm^{-1}) for the rigid DMA molecule is reduced to ∼0.90 kcal/mol (300 cm^{-1}) when the NR_2 inversion is allowed.

For other complexes, with the exception of A-DMOT, similar configurations as those of minima (1) and (2) of A-DMA with slightly modified geometry and interaction energies correspond respectively to the deepest minima (1) and (2) and show high occurrences.

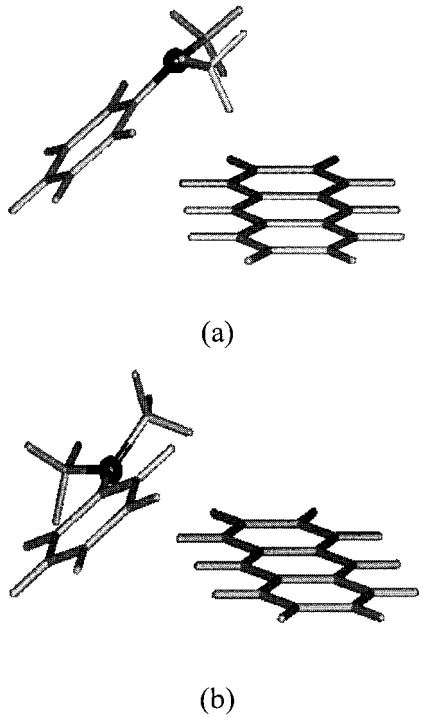

Figure 5. Configurations of the anthracene−dimethylaniline complex corresponding to (a) the most stable minimum and (b) to minimum (2) of the ground-state PES.

The configuration (1) of the A-DMPT complex has practically the same geometry, the same total energy and its partition as the configuration (1) of A-DMA. In A-DMMT, the configu-

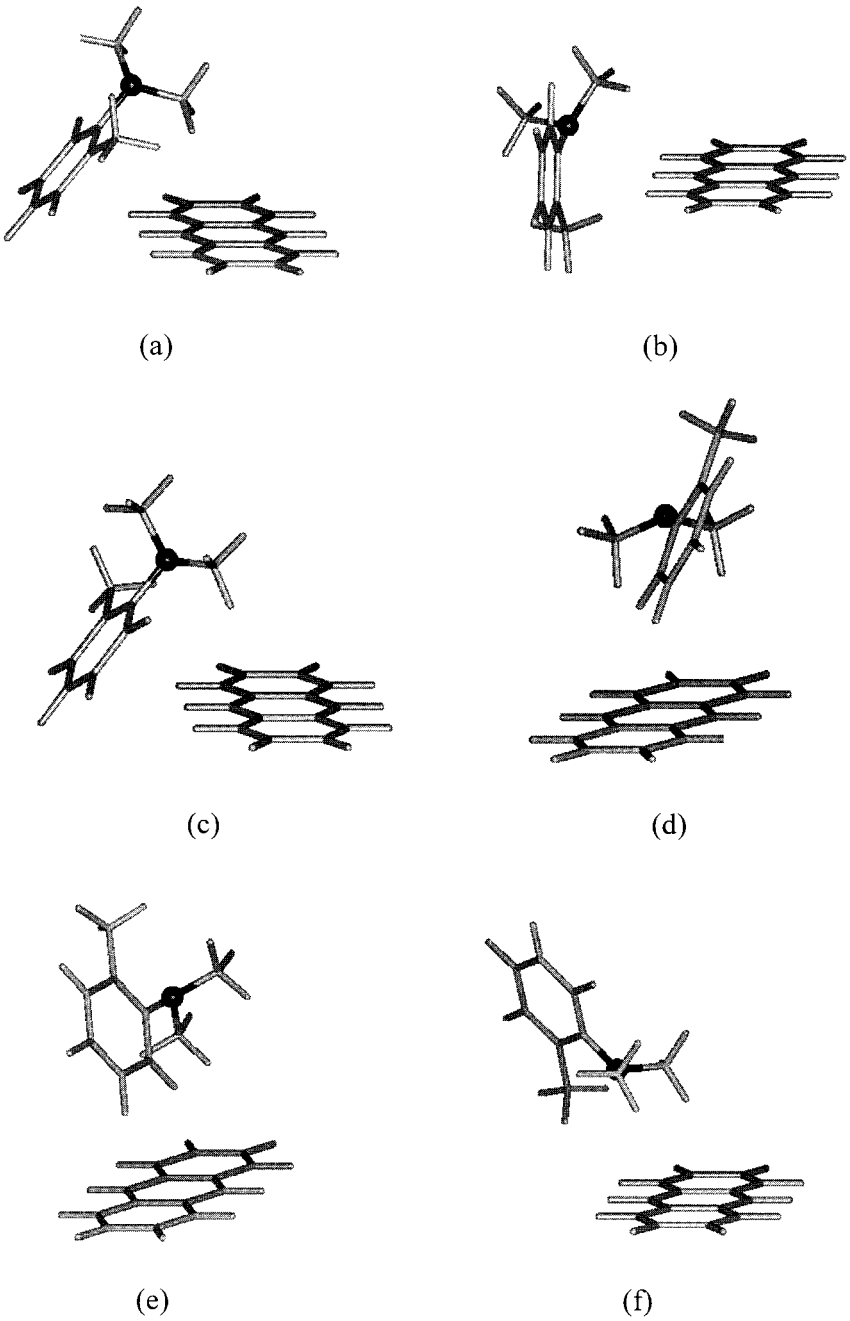

Figure 6. Configurations of the anthracene−dimethyl-*o*-toluidine complex corresponding to (a) minimum (1), (b) minimum (2), (c) minimum (3), (d) minimum (4), (e) minimum (5), and (f) minimum (6) of the ground-state PES.

ration (1) is stabilized by ca. 0.2 kcal/mol, the difference being due to an increase of the dispersion term. The geometry and the total interaction energy of the configuration (1) of the A-DEA complex are nearly identical as in A-DMA. However, individual components of the total interaction energy are different: an increase of the dispersion term (due to a stronger interaction with ethyl instead of methyl groups) compensates a decrease of the electrostatic term. Stabilization of the configuration (2) in A-DMMT and A-DMPT complexes involves a larger dispersion term. As in the A-DMA complex, the $2 \rightarrow 1$ barriers are high but should be reduced if the intramolecular NR_2 inversion is involved.

The case of A-DMOT complex is different. The geometries of minima (1) and (2), apparently similar to those of other complexes, are modified because of the peculiar structure of DMOT. In the configuration (1), only one methyl of the NR_2 group points toward the anthracene molecule, the distance between the N-atom and anthracene molecule is increased to 4.9 Å and the angle between the *L*-axis of DMOT and the plane of the anthracene molecule is increased by 10° (Figure 6a). The interaction energy is reduced by 0.15−0.30 kcal/mol with respect to other complexes, and this reduction essentially results from the decrease of the electrostatic term. The configuration (2) differs from that of other complexes by the value of the angle formed by the two short axes *M* and *M′* which vary from 40°−90° (Figure 6b). The $2 \rightarrow 1$ barrier is equal to 2.32 kcal/mol. Note also that the occurrences of the minima (1) and (2) are not much larger than those of the other ones.

In the case of A-DMA, the minima (3), T-shaped with nearly parallel long axes of both molecules, and (4), with configuration differing from (1) only by the A← orientation of the amino group, are discarded because of their low bonding energies and negligible occurrences. For the A-DEA and A-DMMT complexes, the structure (3) is stabilized and shows a nonnegligible

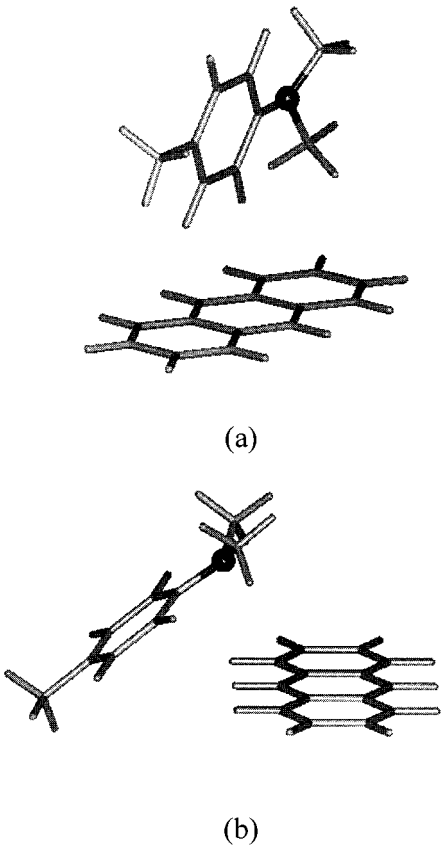

Figure 7. Configurations of the anthracene-dimethyl-p-toluidine complex corresponding to (a) minimum (3) and (b) minimum (4) of the ground-state PES.

occurrence. In spite of its low interaction energy, it may correspond to stable isomeric forms of these complexes.

For the A-DMA complex, the number of selected minima is in agreement with the observation of two isomers, while for the other complexes, with the exception of A-DMOT, the number of selected minima is higher than the number of the observed isomers. As for these latter complexes, the minima (1) and (2) correspond to stable isomeric forms; it would then be necessary to make a choice between the other minima. The choice between minima (3) and (4) of A-DMPT, (3) and (4) of A-DMMT (minimum (5) being eliminated on the basis of its low stability and occurrence), and (3), (4), and (5) of A-DEA is arbitrary. The main parameters of these minima are given in Table 4. Their geometry and those of minima (3), (4), and (5) of A-DMOT are represented in Figures 6−9.

IV. Discussion

A. Number of Isomers. Both theoretical and experimental results show the existence of isomers for all complexes. We found experimentally two isomers for A-DMA complex, three isomers for A-DMPT and A-DMMT complexes, four isomers for A-DEA complex, and six for the A-DMOT complex. The respective number of significant minima is: two, three, five, five, and five. The number of isomers and of significant minima is in relatively good agreement in spite of the difficulty of a choice of the significant ones among all minima found on the complicated potential energy surface.

The experiment shows that the modification of the donor either by methyl substitution in the benzene ring or by replacement of $-CH_3$ by $-C_2H_5$ in the NR_2 group leads to an increase of the number of the *R*-isomers. This observation is confirmed by the modeling since the number of minima in the same energy range increases when DMA is modified by substitution.

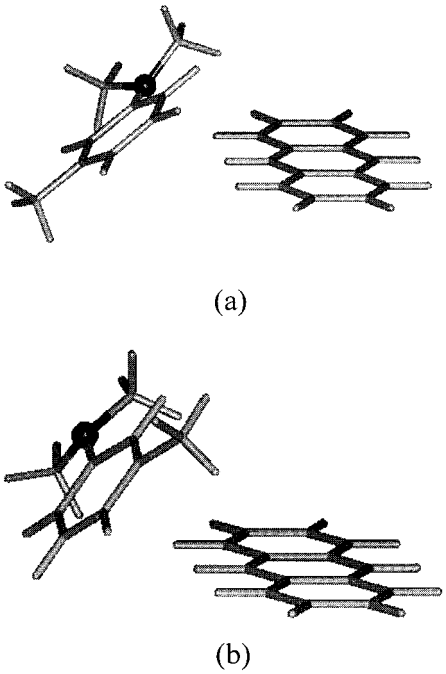

Figure 8. Configurations of the anthracene−dimethyl-*m*-toluidine complex corresponding to (a) minimum (3) and (b) minimum (4) of the ground-state PES.

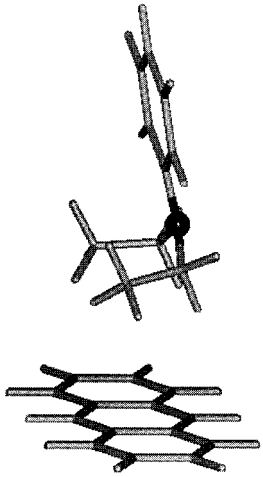

Figure 9. Configuration of the anthracene−diethylaniline complex corresponding to the minimum (4) of the ground-state PES.

B. Effects of the Donor Structure. The para and meta methyl substitution and lengthening of alkyl chains induce relatively small modifications of the donor structure. They will stabilize only such configurations for which the methyl substituent or alkyl chains approach closely and directly interact with the anthracene molecule. This effect appears clearly in the case of the configurations (1) and (2) of the A-DMMT complex stabilized by ∼0.25 and ∼0.55 kcal/mol, respectively. In both cases, the methyl group comes closely to the acceptor ring and the dispersion term is significantly increased. On the other hand, the configuration (3) (Figure 8a) with methyl group at the opposite site of the DMMT molecule has almost exactly the same energy as the configuration (2) of DMA.

One can explain in the same way stabilization of configurations (2) of the A-DMPT and (3) of the A-DEA complexes. On the other hand, the total interaction energy remains unchanged

for the configurations where the methyl group or alkyl chains do not interact with the anthracene molecule: (1), (3) (Figure 7a), and (4) (Figure 7b) of the A-DMPT, and (5) of A-DEA complexes. Moreover, if the para methyl substitution has no effect, the meta methyl substitution and alkyl chains lengthening also results in the appearance of new configurations corresponding to deep minima: (3) and (4) of the A-DMMT (Figure 8a,b) and (4) of A-DEA (Figure 9).

The ortho methyl substitution results in strong deviation of the donor from the planar structure (out of plane rotation of ∼80° of the whole $-NR_2$ group) so that the two methyl of the NR_2 group are no more equivalent. The consequence of this symmetry breakdown is a modification of the configurations (1) and (2) and the appearance of new stable configurations (Figure 6d−f). This result is in good agreement with the experimental data showing a large number of isomeric forms and a nontypical population distribution (unusually weak absorption assigned to the E isomer).

The study limited to the ground-state potential energy surface does not supply sufficient information to establish a nonambiguous relationship between calculated configurations and observed spectra. It shows, however, that for this kind of complexes involving relatively large aromatic molecules; (i) the number of isomers may be large, (ii) the numbers differ strongly between complexes whose donors have slightly different properties, all being simple dimethylaniline derivatives; and (iii) that the stable configurations do not correspond to the simple structures (T-shaped, stacked etc.) suggested by the "chemical intuition". This indicates that one must be very cautious when trying to deduce the complex structures only on the basis of the analogies between the properties of their components. The low symmetry of these systems is consistent with their spectra showing a large number of active external modes (i.e., absence of rigorous selection rules).

References and Notes

(1) Beens, H.; Knibbe, H.; Weller, A. *J. Chem. Phys.* **1967**, *47*, 1183.

(2) Knibbe, H.; Röllig, K.; Schäfer, F. P.; Weller, A. *J. Chem. Phys.* **1967**, *47*, 1184.

(3) Syage, A.; Felker, P. M.; Zewail, A. H. *J. Chem. Phys.* **1984**, *81*, 2233.

(4) van Dantzig, N. A.; Shou, H.; Alfano, J. C.; Yang, N. C.; Levy, D. H. *J. Chem. Phys.* **1994**, *100*, 7068.

(5) Kurono, M.; Takasu, R.; Itoh, M. *J. Phys. Chem.* **1995**, *99*, 9668.

(6) Piuzzi, F. *Chem. Phys. Lett.* **1993**, *209*, 484.

(7) Piuzzi, F.; Brenner, V.; Millié, Ph.; Tramer, A. *J. Photochem. Photobiol. A* **1994**, *80*, 95.

(8) Kaziska, A. J.; Shchuka, M. I.; Wittmeyer, S. A.; Topp, M. R. *J. Phys. Chem.* **1990**, *94*, 767.

(9) Lahmani; Zehnacker-Rentien, A.; Bréhéret, E. *J. Phys. Chem.* **1990**, *94*, 8767.

(10) Chakraborty, T. P.; Lim, E. C. *J. Phys. Chem.* **1993**, *97*, 11151.

(11) Law, K. S.; Schauer, M.; Bernstein, E. R. *J. Chem. Phys.* **1984**, *81*, 4871.

(12) Schmidt, M.; Lecalvé, J.; Mons, M. *J. Chem. Phys.* **1993**, *98*, 6102 and references therein.

(13) Scherzer, W.; Selzle, H. L.; Schlag, E. W. *Chem. Phys. Lett.* **1992**, *195*, 11.

(14) Lipert, R. J.; Colson, S. D. *J. Phys. Chem.* **1989**, *93*, 3894.

(15) (a) Claverie, P. *Intermolecular Interaction: From Diatomic to Biopolymers*, Pullman, B., Ed.; Wiley: New York, 1978; p 69. (b) Langlet, J.; Claverie, P.; Boeuvre, P.; F. J. C. *Int. J. Quantum Chem.* **1981**, *20*, 299.

(16) Brenner, V.; Millié, P. *Z. Phys. D* **1994**, *30*, 327.

(17) Hess, O.; Caffarel, M.; Langlet, J.; Caillet, J.; Huiszoon, C.; Claverie, P. In *Proceedings of the 44th International Meeting of Physical Chemistry on Modeling of Molecular Structure*; Rivail, J. L., Ed.; Elsevier: Amsterdam, 1990.

(18) Vigné-Maeder, F.; Claverie, P. *J. Chem. Phys.* **1988**, *88*, 4934.

(19) Hehre, W. J.; Steward, R. F.; Pople, J. A. *J. Am. Chem. Soc.* **1969**, *51*, 2657.

(20) Dupuis, M.; Rys, J.; King, W. F. *J. Chem. Phys.* **1975**, *65*, 111 (Program 338, QCPE, Chemistry Department, University of Bloomington: Indiana).

(21) Dewar, M. J. S.; Zoebisch, E. G.; Healy, E. F.; Stewart, J. P. *J. Am. Chem. Soc.* **1985**, *107*, 3902.

(22) (a) Brenner, V.; Zehnacker-Rentien, A.; Lahmani, F.; Millié, Ph. *J. Phys. Chem.* **1993**, *97*, 10570. (b) Brenner, V.; Martrenchard, S.; Millié, Ph. Jouvet, C.; Lardeux-Dedonder, C.; Solgadi, D. *J. Phys. Chem.* **1995**, *99*, 5848. (c) Desfrancois, C.; Abdoul-Carime, H.; Khelifa, N.; Scherman, J. P.; Brenner, V.; Millié, Ph. *J. Chem. Phys.* **1995**, *102*, 4952.

(23) (a) Kirkpatrick, S.; Gellet, C. D.; Vecchi, M. P. *Science* **1983**, *220*, 671. (b) Kirkpatrick, S. *J. Stat. Phys.* **1984**, *34*, 975.

(24) (a) Fletcher, R. *Comput. J.* **1963**, *6*, 163. (b) Goldfarb, D. *Math. Comput.* **1970**, *24*, 23. (c) Shanno, D. F. *Math. Comput.* **1970**, *24*, 647.

(25) Bockish, F.; Liotard, D.; Rayez, J. C.; Duguay, B. *Int. J. Quantum Chem.* **1992**, *44*, 619.

(26) Metropolis, N.; Rosenbluth, A.; Rosenbluth, M.; Teller, A.; Teller, E. *J. Chem. Phys.* **1953**, *21*, 1087.

(27) (a) Liotard, D.; Penot, J. P. In *Numerical Methods in the Study of Critical phenomena*; Della, J., Ed.; Springer-Verlag: Berlin, 1981, p 213. (b) Liotard, D. A. *Int. J. Quantum Chem.* **1992**, *44*, 723.

(28) Piuzzi, F.; Tramer, A. *Chem. Phys. Lett.* **1990**, *166*, 503.

(29) (a) Weersink, R. A.; Wallace, S. C. *J. Phys. Chem.* **1993**, *97*, 6127. (b) Weersink, R. A.; Wallace, S. C.; Gordon, R. D. *J. Chem. Phys.* **1995**, *103*, 9530.

(30) Kurbatov, B.; Vilesov, F.; Terenin, A. *Dokl. Akad. Nauk. SSSR* **1961**, *140*, 797. (English translation: *Soviet Phys. Dokl.* **1962**, *6*, 883.)

(31) Lias, S. G.; Jackson, J. A.; Argentar, H.; Liebman, J. F. *J. Org. Chem.* **1985**, *50*, 333.

(32) Maier, J. P.; Turner, D. W. *J. Chem. Soc. Faraday Trans. 2* **1973**, *69*, 521.

(33) (a) Lister, D. J.; Tyler, J. K.; Hog, J. H.; Larsen, N. W. *J. Mol. Struct.* **1974**, *23*, 253. (b) Fukuyo, M.; Hirotsu, K.; Higuchi, T. *Acta Crystallogr., Sect. B* **1982**, *38*, 643.

(34) Gorse, A. D.; Pesquer, M. *J. Mol. Struct.* (*THEOCHEM*) **1993**, *281*, 21.

(35) Cervellati, R.; Dal Borgo, A.; Lister, D. G. *J. Mol. Struct.* **1982**, *78*, 161.

(36) In our previous paper[31] on the A-DEA complex, we were unable to explain the complicated vibrational structure of its excitation spectrum supposed to be due to a single species. In fact, this structure is due to the overlapping of relatively simple absorption spectra of three isomers.